ARCHIVES OF ELECTRICAL ENGINEERING VOL. 61(4), pp. 499-515 (2012)

DOI 10.2478/v10171-012-0039-6

Modeling, simulation and experimental analysis of permanent magnet brushless DC motors for sensorless operation

E. KALIAPPAN, C. CHELLAMUTHU

Electrical and Electronics Engineering
R.M.K. Engineering College
Chennai, India

e-mail: kali_eee05@yahoo.com, malgudi60@hotmail.com

(Received: 12.01.2011, revised: 24.04.2012)

Abstract: This paper presents a simplified modeling, simulation and Experimental analysis of permanent magnet brushless dc motors (PMBLDC) for sensorless operation. This model provides a mechanism for monitoring and controlling of voltage, current, speed and torque. The sensorless scheme employs direct back emf based zero crossing detection for controlling the dynamic characteristics.

Key words: PMBLDC motor, modeling, simulation, sensorless operation, back emf zero cross point

1. Introduction

In the literature there are several simulation models available for BLDC motor drives. These models employ state-space equations, Fourier series or d-q axis model. Even though these models have made a great contribution in the BLDC motor drives, there is no comprehensive model for the analysis of motor used in sensorless operation [1]. The machine models are often transformed to a rotating reference frame to simplify and to improve the computational efficiency. But, this approach will not improve the computational efficiency because the d-q transformations are suitable only for machines with sinusoidal voltage as discussed [2]. The PMBLDC motors are normally powered by conventional three phase voltage source inverters (VSI) or current source inverters (CSI) which are controlled based on the rotor position information obtained from hall sensors, resolvers or absolute position sensors. But these position sensors have numerous drawbacks like increase in cost, complexity in control, temperature sensitivity requiring special arrangements. These sensors reduce the system reliability and acceptability. Therefore, sensorless techniques have become a subject of great interest in recent times. A number of sensorless techniques have been developed for PMBLDC motor. Some of the techniques presented [3] in the literature are based on position sensing using back emf zero detection crossing, terminal voltage sensing, sensing third harmonics of the motional

emf, integration of the back emf, position sensing using inductance variation, position sensing based on flux linkage variation, Extended Kalman filter estimation or detecting the free-wheeling diode conduction in open phase [4, 5].

In PMBLDC motors, only two out of three phases are excited at any time leaving the third winding floating. The back emf in the floating winding can be measured to determine the switching sequence for commutation of power switching devices in the 3 phase inverter. The terminal voltage of the floating winding with respect to the neutral point of motor is needed to get the zero crossing time of the back emf. The sensorless control technique based on Zero Cross Point (ZCP) of the back emf has been widely used for low cost an application is proposed by J. Shao [6]. In the ZCP method the back emf cannot be obtained when the BLDC motor is at standstill or operating nearly zero speed as discussed by Yen-Shin Lai and Yong-kai Lin [7]. Therefore, a special starting control is needed for smooth starting and reliable transfer to sensorless control [8].

In this paper a Matlab/Simulink model of PMBLDC motor suitable for Sensorless operation is developed. Using this model, the dynamic behavior of the motor is studied. Also simulation has been carried out to study the effectiveness of the sensorless control using direct back emf detection. The rest of the paper is organized as follows: Section 2 presents the Modeling of PMBLDC motor with sensorless control using Matlab/Simulink. Section 3 and 4 presents the simulation and experimental results of the proposed method and in Section 5, the conclusion are discussed.

2. Modeling of PMBLDC motor for sensorless operation

A three phase star connected BLDC motor driven by a three phase inverter using six step commutations is considered for the study. Figure1 shows the simplified BLDC motor drive scheme and Figure 2 gives Ideal current and back-emf waveforms with hall signals. The conducting interval of each phase is 120 electrical degrees. The commutation instant is determined in every sixty electrical degrees by detecting the back emf's zero crossing point of the floating phase. Only two phases conduct current at any time, leaving the third phase open which is available for measuring the back emf.

The analysis is based on the following assumptions

1) Stator resistance of all the windings are equal, self and mutual inductance are constant.
2) The motor is not saturated.
3) Iron losses are negligible.
4) Semiconductor switches are ideal.

2.1. PMBLDC motor modeling

The voltage equations of BLDC motor shown in Figure (1) are derived as

$$v_{ab} = R(i_a - i_b) + L\frac{d}{dt}(i_a - i_b) + e_a - e_b \ , \tag{1}$$

$$v_{bc} = R(i_b - i_c) + L\frac{d}{dt}(i_b - i_c) + e_b - e_c, \tag{2}$$

$$v_{ca} = R(i_c - i_a) + L\frac{d}{dt}(i_c - i_a) + e_c - e_a\ , \tag{3}$$

where R – stator resistance per phase, L – stator inductance per phase, i_a, i_b and i_c – instantaneous stator phase currents, v_{ab} $v_{bc} v_{ca}$ – instantaneous stator line voltages, e_a, e_b and e_c – instantaneous phase back – emfs.

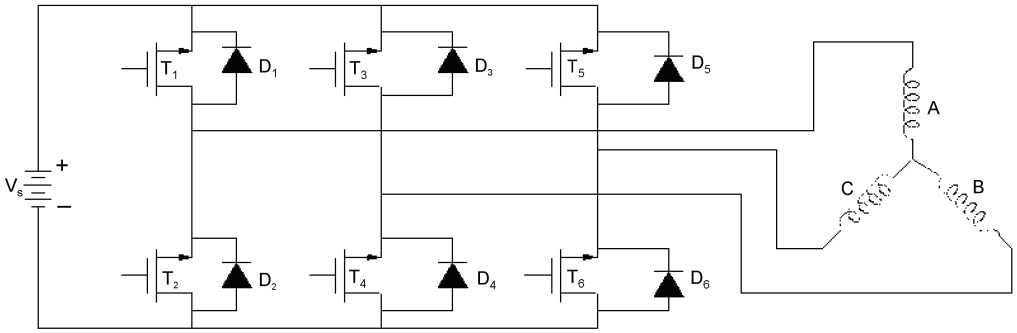

Fig. 1. Basic PMBLDC motor Drive scheme

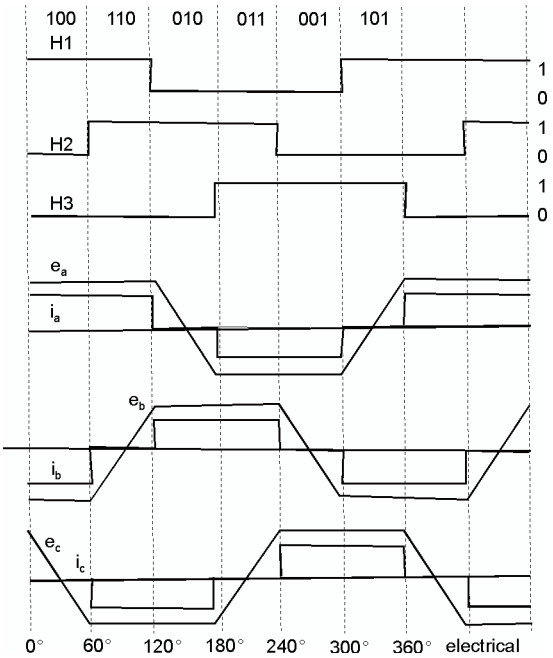

Fig. 2. Ideal current and back-emf waveform with hall the signals

The current relationship is given by

$$i_a + i_b + i_c = 0. \tag{4}$$

Equation (4) is rewritten as

$$i_c = -(i_a + i_b). \tag{5}$$

Substituting Equation (5) in Equation (1) and Equation (2),
Using Equation (5) the line voltage equations are rearranged as

$$v_{ab} = R(i_a - i_b) + L\frac{d}{dt}(i_a - i_b) + e_a - e_b, \tag{6}$$

$$v_{bc} = R(i_a + 2i_b) + L\frac{d}{dt}(i_a + 2i_b) + e_b - e_c. \tag{7}$$

The back emf depends on flux of the permanent magnet rotor and the speed of the rotor, which is given as

$$\begin{bmatrix} e_a \\ e_b \\ e_c \end{bmatrix} = \frac{k_e w_m}{2} \begin{bmatrix} F(\theta_e) \\ F\left(\theta_e - \frac{2\Pi}{3}\right) \\ F\left(\theta_e - \frac{4\Pi}{3}\right) \end{bmatrix} \tag{8}$$

The generated electromagnetic torque is given by Equation (9)

$$T_e = \left[\frac{K_t}{2}F(\theta_e)i_a + \frac{K_t}{2}F\left(\theta_e - \frac{2\Pi}{3}\right)i_b + \frac{K_t}{2}F\left(\theta_e - \frac{4\Pi}{3}\right)i_c\right], \tag{9}$$

The dynamics of the motor and load are expressed as

$$T_e = K_f w_m + J\frac{d}{dt}(w_m) + T_L, \tag{10}$$

$$T_e - T_L = K_f w_m + J\frac{d}{dt}(w_m), \tag{11}$$

$$J\frac{d}{dt}(w_m) = T_e - T_L - K_f w_m, \tag{12}$$

$$w_m^{'} = -\frac{k_f}{J}w_m + \frac{1}{J}[T_e - T_L], \tag{13}$$

$$\theta_m^{'} = w_m. \tag{14}$$

where $\theta_e = p/2\theta_m$ electrical angle, degrees; w_m = rotor speed, rad/sec; k_e = back-emf constant, volts/rad/sec; J = moment of inertia, kg/m^2; k_f = friction constant, Nm/rad/sec; T_L = load torque, Nm; k_t = torque constant, Nm.

2.2. Inverter modeling

Inverter and the switching sequence are modeled using S-function. Table 1 shows the switching sequence, current direction and the position signals. At any instant of time, one of the phases is open. Zero crossing of the open phase back emf is detected to get the rotor position. Let us consider an instant where phases A and B are in conduction and phase C is open. The ZCP of phase C is used to trigger a switch in a phase A or B which is more positive with respect to the neutral point.

The triggering sequence generated by the ZCP of the back emf of the open phase is similar to the one produced by the hall sensors mounted on the machine. There are six states in a cycle of operation. The values of voltages and current are given for the state 1.

State 1. (0-60°): Commutation period: The phases A and B are conducting and phase c is freewheeling through diode D5,

$$\begin{aligned} &\text{For } i_c \neq 0 \\ &v_{ab} = V_s \\ &v_{bc} = 0 \\ &v_{ca} = -V_s. \end{aligned} \tag{15}$$

ON period: Phases A and B carry current and C phase is open

$$\begin{aligned} &\text{For } i_c = 0 \\ &v_{ab} = V_s \\ &v_{bc} = \frac{1}{2}(-V_s + e_a + e_b - 2e_c) \\ &v_{ca} = \frac{1}{2}(-V_s - e_a - e_b + 2e_c). \end{aligned} \tag{16}$$

$$\begin{aligned} &\text{For } i_c \neq 0 \\ &u_{ab} = v_{ab} - (e_a - e_b) = V_s - e_a + e_b \\ &u_{bc} = v_{bc} - (e_b - e_c) = -e_b + e_c \\ &u_{ca} = v_{ca} - (e_c - e_a) = -V_s - e_c + e_a. \end{aligned} \tag{17}$$

State 2. (60-120°):

$$\text{For } i_b \neq 0 \quad v_{ab} - e_{ab} = -e_a + e_b, \quad v_{bc} - e_{bc} = V_s - e_b + e_c. \tag{18}$$

$$\text{For } i_b = 0 \quad v_{ab} - e_{ab} = \frac{1}{2}(V_s - e_a + e_c), \quad v_{bc} - e_{bc} = \frac{1}{2}(V_s - e_a + e_c). \tag{19}$$

State 3. (120-180°):

$$\text{For } i_a \neq 0 \quad v_{ab} - e_{ab} = -V_s - e_a + e_b, \quad v_{bc} - e_{bc} = V_s - e_b + e_c. \tag{20}$$

$$\text{For } i_a = 0 \quad v_{ab} - e_{ab} = \frac{1}{2}(-V_s + e_b - e_c), \quad v_{bc} - e_{bc} = V_s - e_b + e_c. \tag{21}$$

State 4. (180-240°):

$$\text{For } i_c \neq 0 \quad V_{ab} - e_{ab} = -V_s - e_a + e_b, \quad V_{bc} - e_{bc} = -e_b + e_c. \tag{22}$$

$$\text{For } i_c = 0 \quad v_{ab} - e_{ab} = -V_s - e_a + e_b, \quad v_{bc} - e_{bc} = \frac{1}{2}(V_s + e_a - e_b). \tag{23}$$

State 5. (240-300°):

$$\text{For } i_b \neq 0 \quad v_{ab} - e_{ab} = -e_a + e_b, \quad v_{bc} - e_{bc} = -V_s - e_b + e_c. \tag{24}$$

$$\text{For } i_b = 0 \quad v_{ab} - e_{ab} = \frac{1}{2}(-V_s - e_a + e_c), \quad v_{bc} - e_{bc} = \frac{1}{2}(-V_s - e_a + e_c). \tag{25}$$

State 6. (300-360°)

$$\text{For } i_a \neq 0 \quad v_{ab} - e_{ab} = V_s - e_a + e_b, \quad v_{bc} - e_{bc} = -V_s - e_b + e_c. \tag{26}$$

$$\text{For } i_a = 0 \quad v_{ab} - e_{ab} = \frac{1}{2}(V_s + e_b + e_c), \quad v_{bc} - e_{bc} = -V_s - e_b + e_c. \tag{27}$$

Where u_{ab}, u_{bc} and u_{ca} are the voltage drops across the impedance consisting of resistance and inductance of the phases and V_s is the dc source voltage Similarly the expressions for the remaining states 2 to 6 are derived and obtained.

Table 1. Switching sequence

Switching interval degree	Sequence number	Position sensor			Switch closed		Phase current		
		H1	H2	H3			A	B	C
(0-60)	0	1	0	0	T1	T4	$+i_a$	$-i_a$	off
(60-120)	1	1	1	0	T1	T6	$+i_a$	off	$-i_c$
(120-180)	2	0	1	0	T3	T6	off	$+i_b$	$-i_c$
(180-240)	3	0	1	1	T3	T2	$-i_a$	$+i_b$	off
(240-300)	4	0	0	1	T5	T2	$-i_a$	off	$+i_c$
(300-360)	5	1	0	1	T5	T4	off	$-i_b$	$+i_c$

3. Simulation results

The Specifications of the BLDC motor used for the simulation are given in Table 2. Equation (1) to (14) has been used to develop a simulation model using S-function in Matlab. Figure 3 shows the complete simulation model of the PMBLDC motor drive consisting of three blocks namely: switching sequence block, inverter block and BLDC motor block.

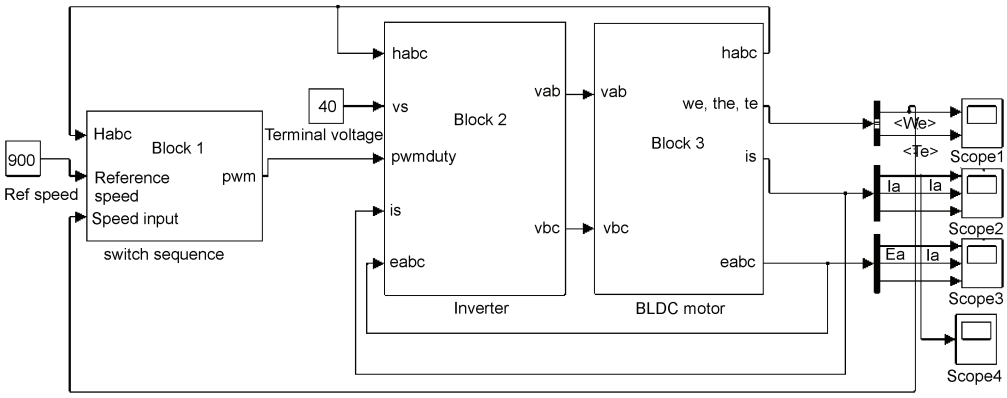

Fig. 3.Complete simulation model of the PMBLDC motor drive

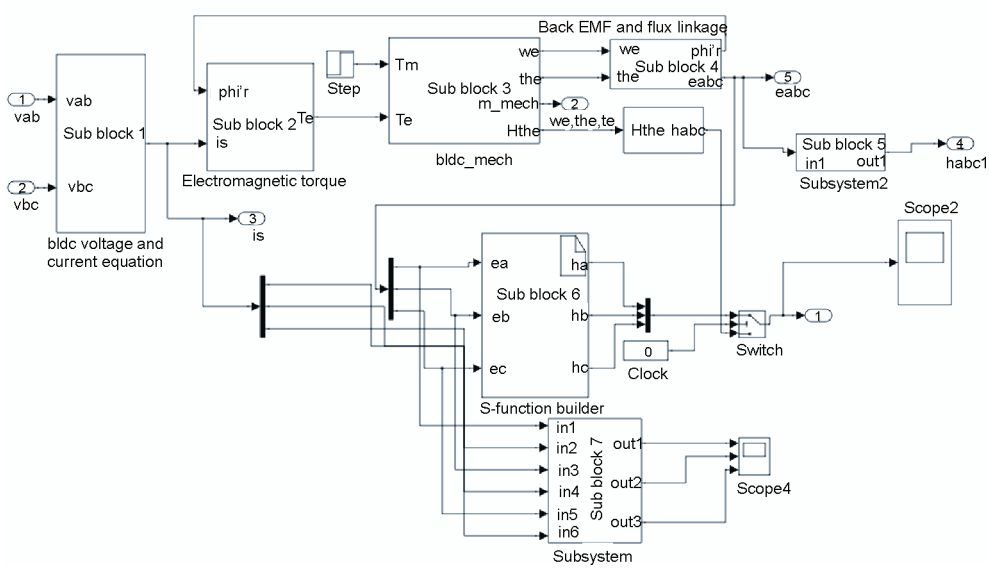

Fig. 4. Sub-blocks of BLDC motor model (Block 3) with back-emf zero cross detection

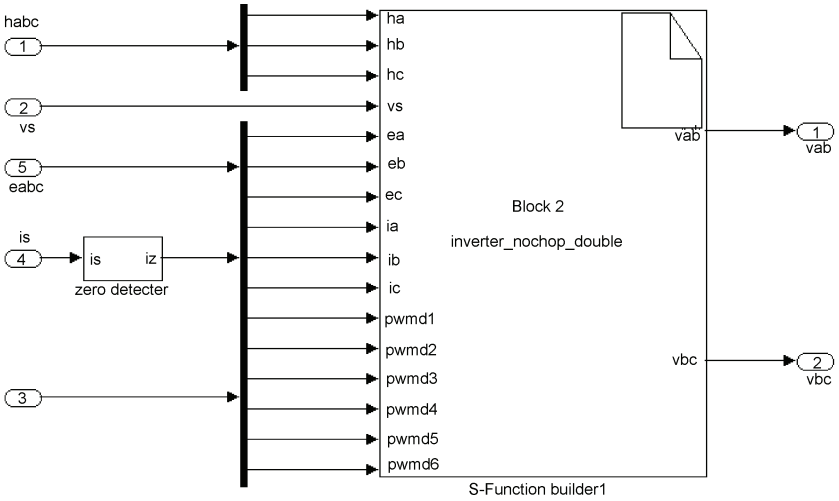

Fig. 5. The inverter S-function builder (Block 2)

The BLDC motor block consisting of seven sub-blocks as labeled in the Figure 4 represents the Equations 1 to 8. Sub-block 1 as shown in Figure 6 represents the BLDC motor's voltage and current equations [Equations 5 and 6] which take the dc voltage v_{ab} and v_{bc} as inputs and gives the phase current, i_s as output. The Sub- block 2 implements Equation 9 using the current output of sub-block 1 as the input along with the flux linkage and produces the electromagnetic torque (T_e) as the output. The Sub-block 3 represents Equations 10 to 14 and are modeled as the mechanical block which takes the electromagnetic torque (T_e) from the sub-block 2 along with the load torque (T_L) as input and gives speed and position as outputs. The Sub-block 4 takes speed and position as input and gives back emf and flux linkages as output as given in Figure 7.

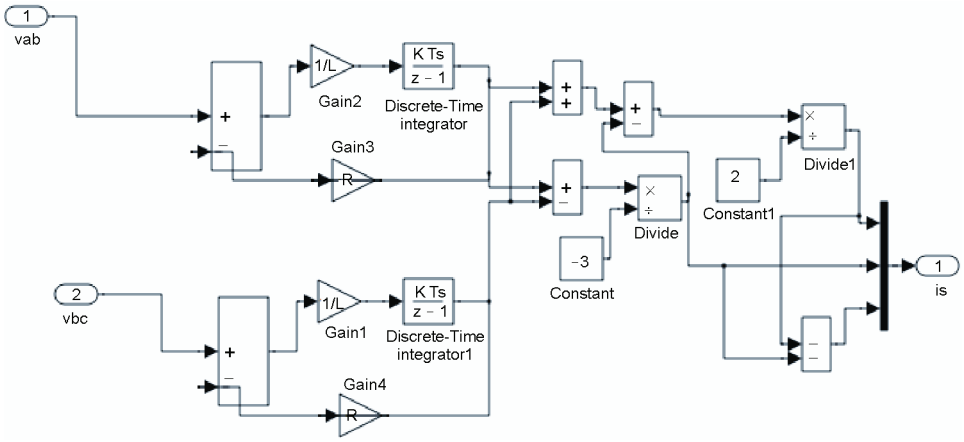

Fig. 6. BLDC voltage and current equations block (Sub-block 1)

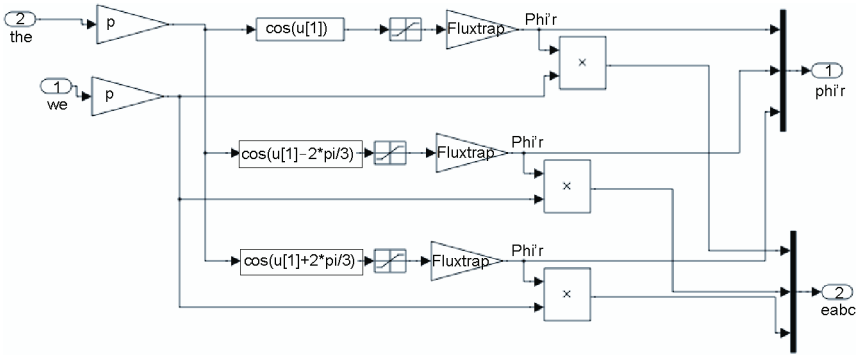

Fig. 7. Generation of back Emf and flux linkage from the rotor position(Sub- block 4)

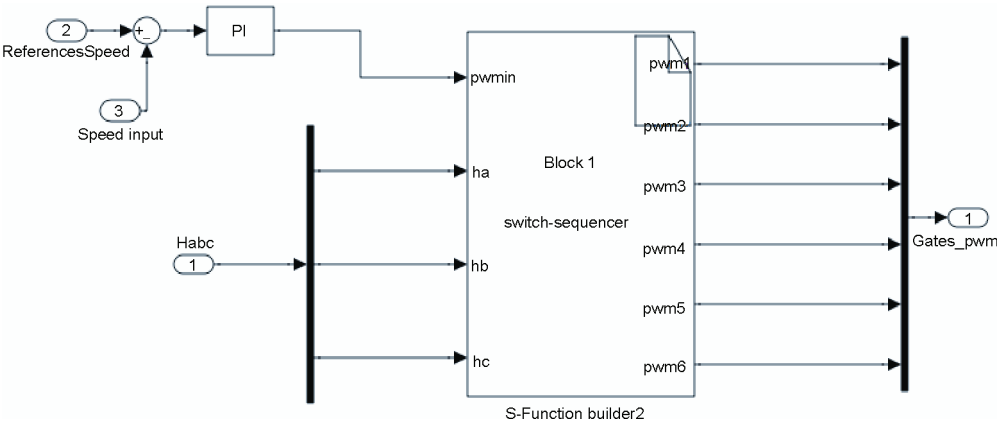

Fig. 8.Generating the switching sequence (Block 1)

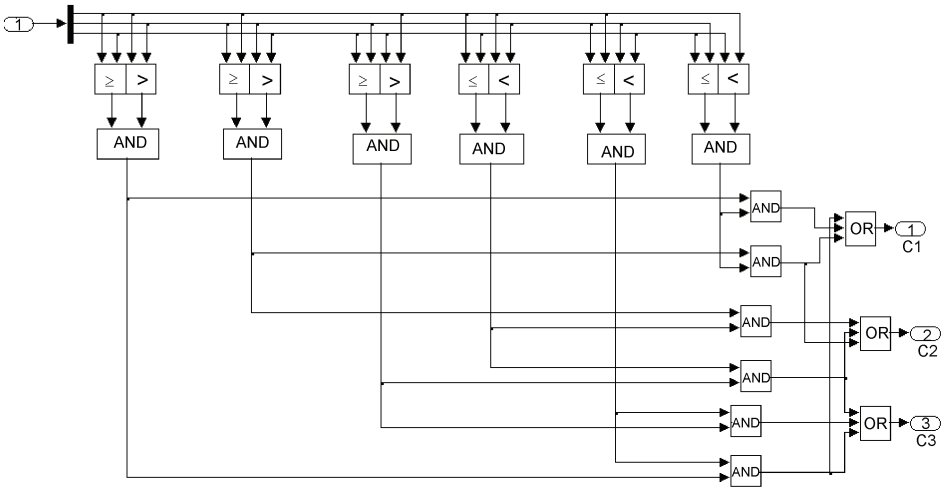

Fig. 9. Back EMF to theta conversion block (Sub-block 5)

Table 2. Motor parameters

Motor parameters	Values
Per phase resistance (R)	0.6 ohm
Per phase Inductance (L)	0.42 mH
Moment of inertia (J)	0.0002 kgm^2
Back Emf Constant (Kb)	0.1 V/rad/sec
Torque Constant(Kt)	0.1 Nm/A
Number of poles	8

This back emf along with the phase current (i_s) are given as inputs to the zero cross detection block (Sub-block 6) as given in Figure 10. Sub-block 5 shown in Figure 9 is the hall sensor block and this is for the open loop control of the BLDC motor during the starting. Sub-block 7 represents the sub system of the zero cross detection circuit which gives the sensorless position information. The inverter and switching logic are implemented as an S-function that takes DC source voltage and the firing sequence as the inputs as shown in Figures 5 and 8.

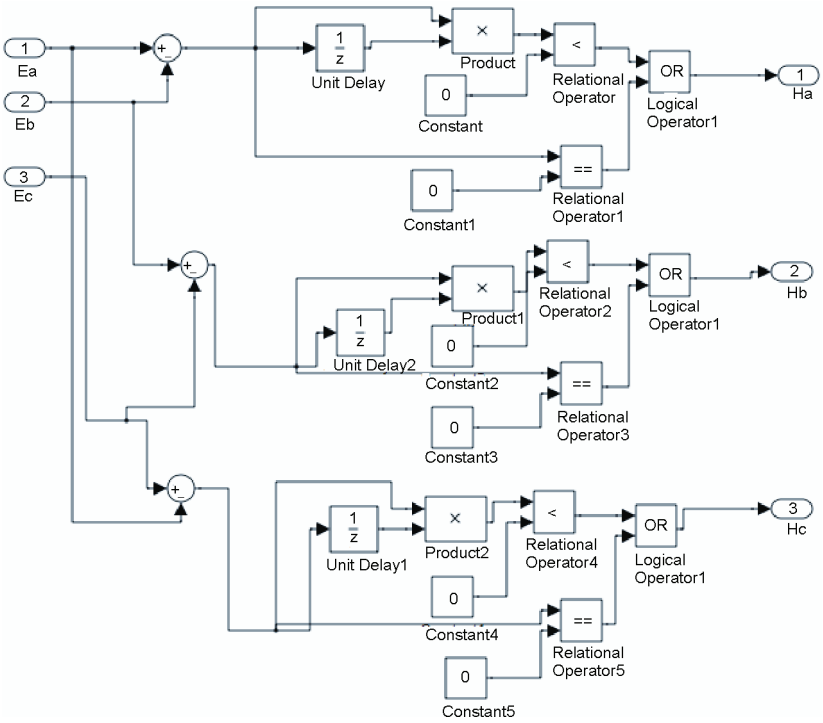

Fig. 10. Zero crossing detection block (Sub-block 6)

The firing signal includes a PWM option for any 60 degree interval. The output voltage of the inverter depends on DC source voltage, rotor position, phase current and also the value

of the back emf. When a switch in a phase is turned off, the outgoing phase current freewheels through the diode where as the incoming phase current increases from Zero to full load value. Position of the rotor decides the incoming and outgoing phases. In this model a hysteresis current control technique is implemented for fast dynamic response during transient states.

This hysteresis current control logic is realized in co-operation with the measured phase current, reference current and rotor position. Based on the hysteresis output the switching functions are determined to model the operation of PWM inverter.

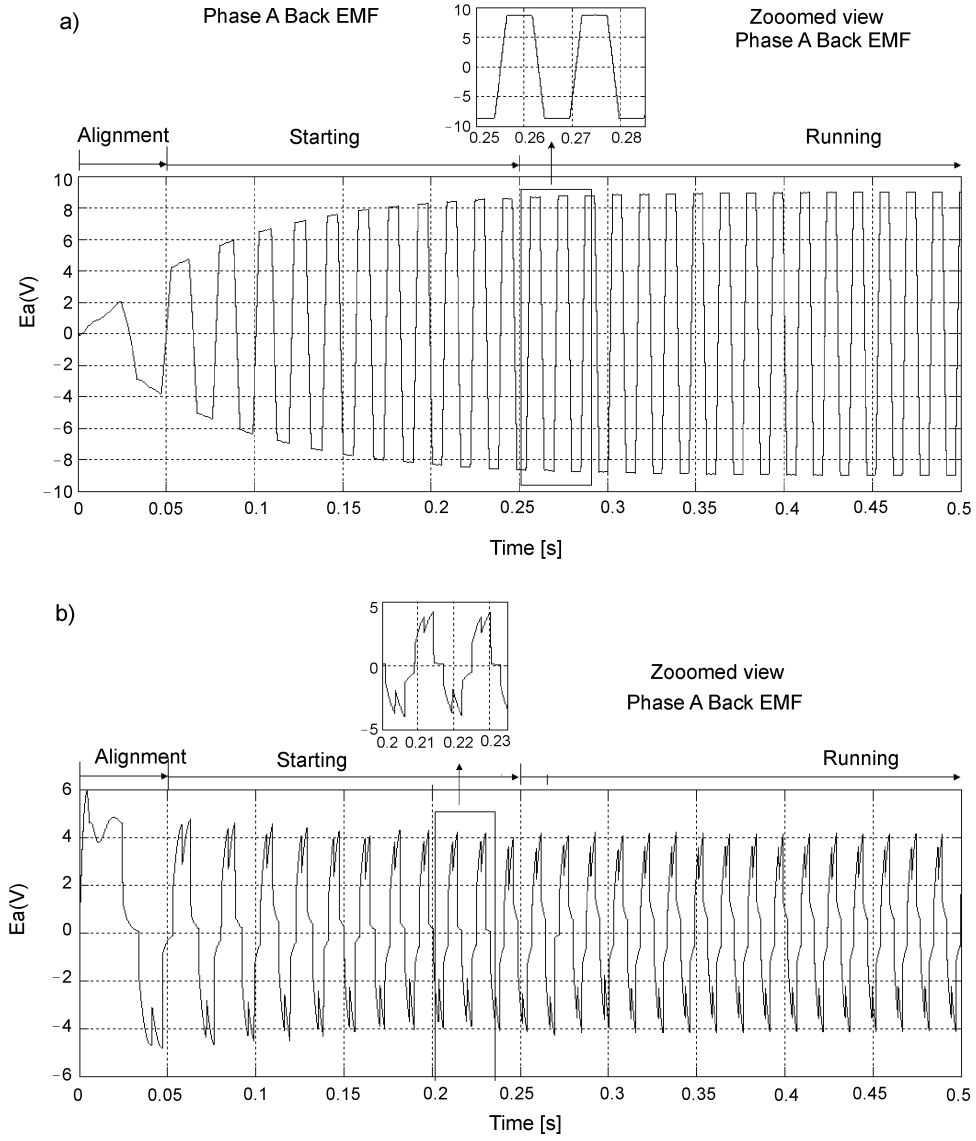

Fig. 11. Generated back emf waveform and phase current waveform from the rotor position

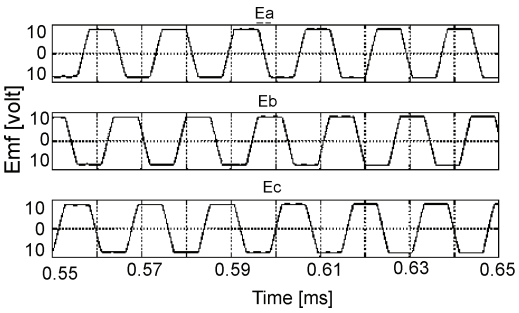

Fig. 12. Generated three phase symmetrical back EMF waveforms from the rotor position

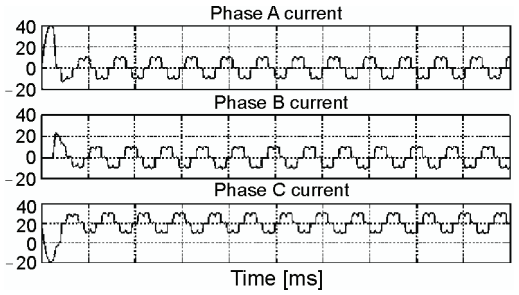

Fig. 13. Generated three phase symmetrical current waveforms from the rotor position

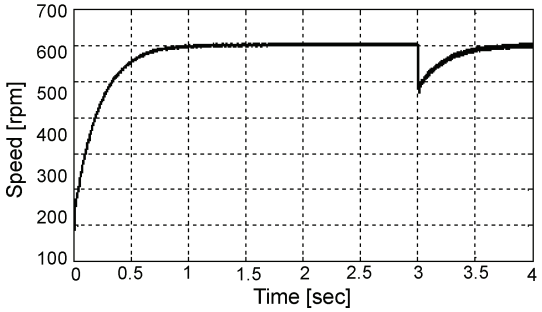

Fig. 14. Speed waveform in rpm

Figure 11 show the simulated back emf waveform and phase current waveforms along with a zoomed view. The simulation model of PM BLDC motor is run for a period of 1 second: the duration between 0 to 0.2 second is the alignment and starting period and the remaining duration is the running period as shown in Figure 11. Figures 12 and 13 shows the generated three phase symmetrical back emf and phase current waveforms. The response of the phase currents when load torque is applied at 0.4 sec is shown in Figure15 along with an enlarged view.

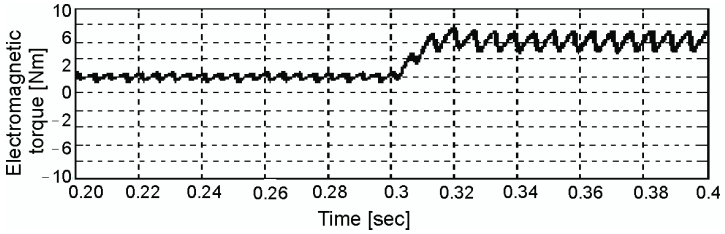

Fig. 15. Electromagnetic torque waveform

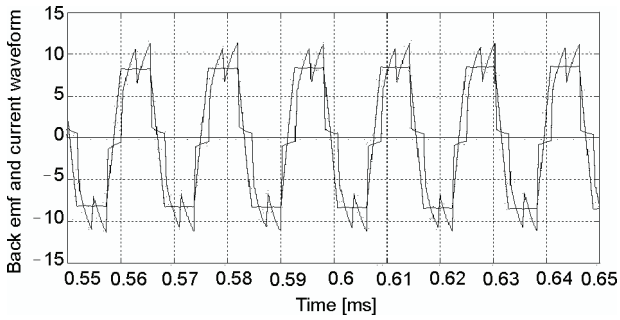

Fig. 16. Zero crossing of Back EMF and Phase current: a) position signal from the backemf zerocrossing; b) position signal from the Hall Signal

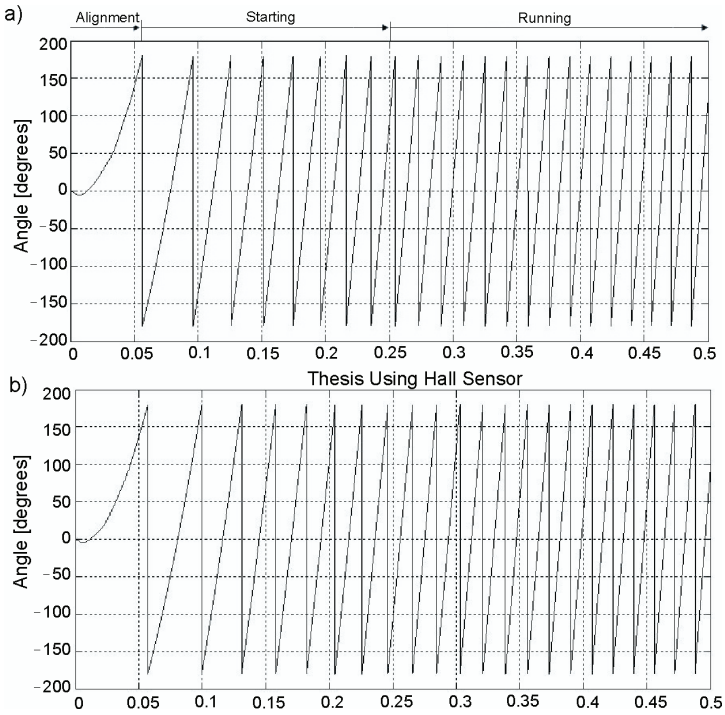

Fig. 17. Comparison of the position signal between the sensorless scheme and hall sensors

Figures 14 and 15 shows the speed and electromagnetic torque waveforms captured when load of 0.5 Nm is applied at 0.3 seconds. The current and back emf of A-phase are monitored and compared to know the zero crossing instants as shown in Figure 16. Figure 17 gives the Comparison of the position signal obtained from the sensorless scheme and hall signals when the motor is loaded. Observing both these figures, we see there is some amount of phase difference, with sensorless mode leading the other.

4. Experimental results

The experimental setup used for the validation of the proposed modeling of BLDC motor for sensorless operation is given in Figure 18. It consists of C0851F310 microcontroller, a 3 phases MOSFET, voltage divider circuit, current amplifier, speed and current controller and three dual gate drivers.

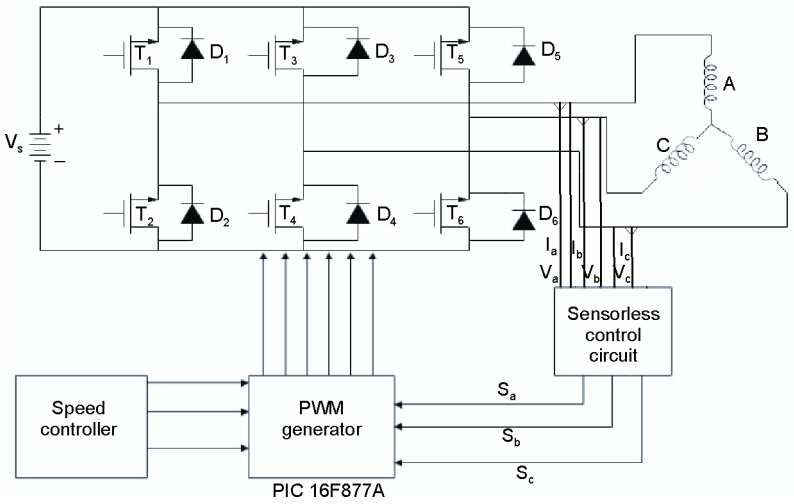

Fig. 18. Block diagram of the experimental setup

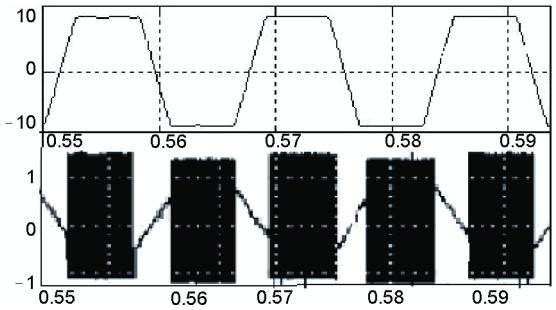

Fig. 19. Back emf waveform with the switching function: a) phase a; b) phase b; c) phase c

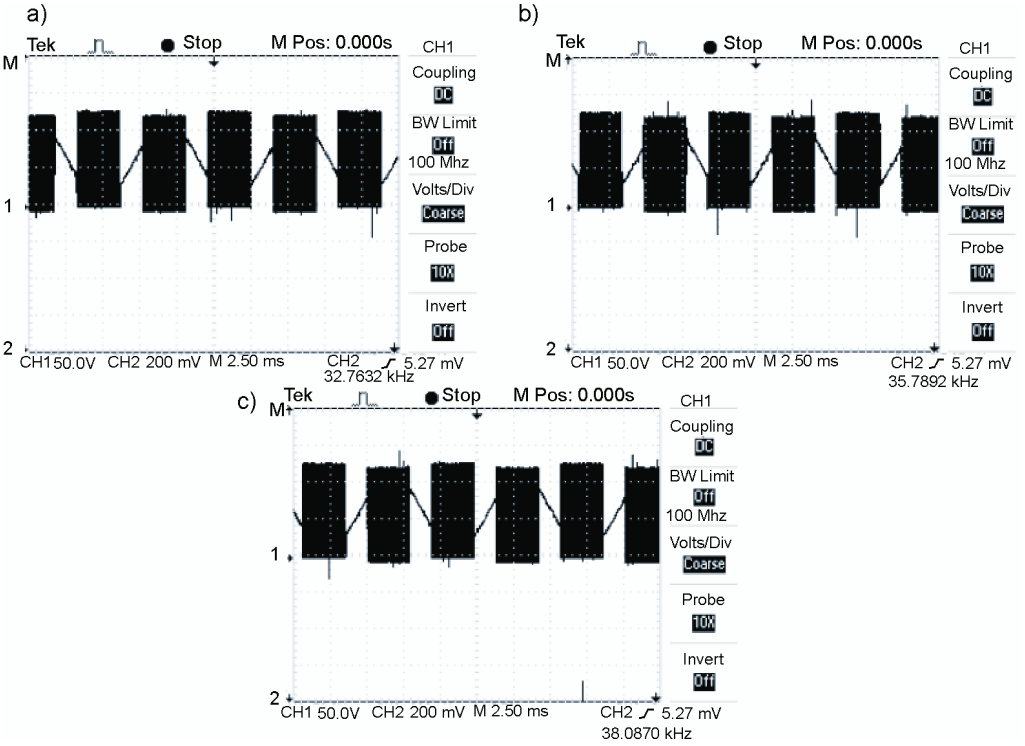

Fig. 20. Switching function of the three phases: phase a), phase b), phase c)

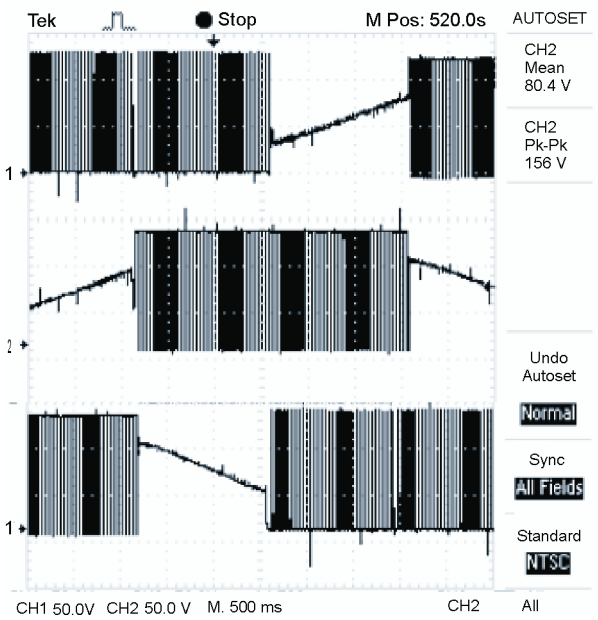

Fig. 21. Enlarged view of line-line voltages of three phases

Three simple resistive divider circuits are connected to the three output phases with the bottom resistor consists of a capacitor in it acting as a RC filter circuit. Motors supply voltage is sensed by connecting a resistive divider circuit across the terminal. Figure 19 shows the switching functions of phase-A with line-line voltage v_{ab} waveforms according to conducting modes. Figure 20 shows the switching functions of three phases. Figure 21 shows the enlarged view of line-line voltages of three phases. Figure 22 shows the measured expanded current of phase-A.

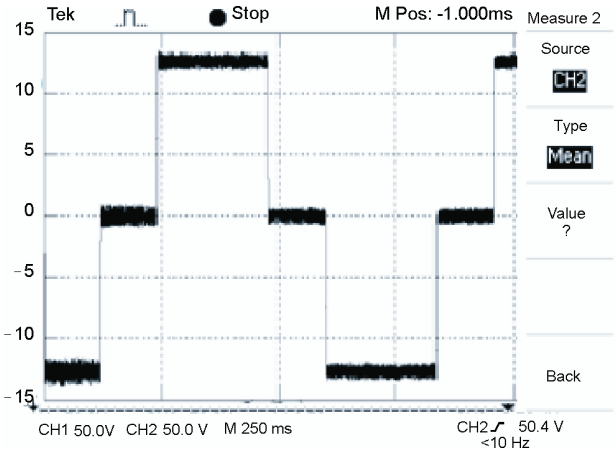

Fig. 22. Measured phase current waveform of phase-A

5. Conclusion

This paper presents a simplified modeling, simulation and experimental analysis of Permanent Magnet brushless dc motors suitable for Sensorless operation using Matlab. The technique of zero crossing of back emf has been used to estimate the rotor position replacing the hall sensors. The voltage and current waveform of the machine were monitored and compared with those obtained using the hall sensors. The results of the sensorless operation matched very closely with those results obtained with hall sensors. This clearly demonstrates that the proposed model for based sensorless control can replace the hall sensor in the PMBLDC drive. This model can be easily extended for the other sensorless control techniques with a small change in the model.

References

[1] Lee B.-K., Ehsani M., *Advanced simulation model for brushless DC Motor drives.* Electric power components and systems, pp. 841-868 (2003).

[2] Luk P.C.K., Lee C.K., *Efficient Modeling of Brushless DC motor drives*. [In:] Industrial Electronics, Control and Instrumentation (1994).

[3] Acarnely P.P., Watson J.F., *Review of position – sensorless operation of brushless permanent – magnet machines*. IEEE Trans. Ind. Electron. 53(2): 352-362 (2006).
[4] Kim D.K., Lee K.W., Kwon B.I., *Commutation torque ripple reduction in a position sensorless brushless DC motor drive.* IEEE Trans. Power Electron. 21(6): 1762-1768 (2006).
[5] Lin C.T., Hung C.W., Liu C.W., *Position sensorless control for four-switch three-phase brushless dc motor drives*. IEEE Trans. Power Electron. 23(1): 438-444 (2008).
[6] Shao J., *An improved microcontroller-based sensorless brushless DC(BLDC) motor drive for automotive applications*. IEEE Trans. Ind. Appl. 42(5): 1216-1222 (2006).
[7] Lai Y.-S. Lin Y.-K., *A unified approach to zero-crossing point detection of back EMF for Brushless DC motor drives without current and hall sensors.* IEEE Trans. Power Electron. 26(6), (2011).
[8] Lee K.W., KimD.K, Kim B.T., Kwon B.I., *A novel starting method of the surface permanent-magnet BLDC motors without position sensor for reciprocating compressor.* IEEE Trans. Power Electron. 44(1): 85-92(2008).